HIGH RESOLUTION IMAGING OF THE SUN WITH CORONAS-I

NASA Grant NAGW-4675

Final Report

For the Period 1 June 1995 through 30 September 1997

Principal Investigator
Dr. Margarita Karovska

March 1998

Prepared for:

National Aeronautics and Space Administration
Washington, D.C.

Smithsonian Institution
Astrophysical Observatory
Cambridge, Massachusetts 02138

The Smithsonian Astrophysical Observatory
is a member of the
Harvard-Smithsonian Center for Astrophysics

The NASA Technical Officer for this grant is W.J. Wagner, Code: SSS, National Aeronautics and Space Administration, Washington, D.C. .

HIGH RESOLUTION IMAGING OF THE SUN WITH CORONAS-I

M. Karovska
Harvard-Smithsonian Center for Astrophysics, Cambridge, MA 02138

ABSTRACT

We applied several image restoration and enhancement techniques, to CORONAS-I images. We carried out the characterization of the Point Spread Function (PSF) using the unique capability of the Blind Iterative Deconvolution (BID) technique, which recovers the real PSF at a given location and time of observation, when limited a priori information is available on its characteristics. We also applied image enhancement technique to extract the small scall structure inbeded in bright large scale structures on the disk and on the limb. The results demonstrate the capability of the image post-processing to substantially increase the yield from the space observations by improving the resolution and reducing noise in the images.

1. Introduction

The CORONAS-I mission, launched in 1993, is first of two missions dedicated to solar observations utilizing the AUOS (Automatic Universal Orbital Station) satellite platform. The CORONAS-I scientific payload includes two imaging instruments: the Multichannel XUV Telescope/Coronagraph (TEREK-C), and the Multichannel XUV Imaging Spectroheliograph (RES-C) (see Oraevsky and Zhugzhda 1991, Zhitnik *et al* 1993). The TEREK-C is a normal-incidence telescope consisting of two XUV channels and a coronagraph channel. The XUV channels consist of (1) high resolution channel (X) for observations in the spectral region centered at 175 *angstrom*, and (2) medium resolution channel (MR) for observations in spectral regions centered at 132, 175 and 304 *angstrom*. The images are recorded using a 1024 x 1156 CCD detector; pixel sizes for the X and MX channels are 1" and 4" respectively. The white line coronagraph has a 516 x 1156 pixel detector with a pixel size of 30". The RES-C instrument provided monochromatic images of the Sun in three spectral regions: 180 - 205 *angstrom* (XUV channel), 8.41 -8.43 *angstrom* (Mg XII channel) and 1.85 -1.87 *angstrom* (Fe XXV channel). The spectral resolution is 0.015 *angstrom*/pixel for the XUV channel, 0.002 *angstrom*/pixel for the Mg XII channel, and 0.0001 *angstrom*/pixel for the Fe XXV, while the angular resolution in all three channels is 4". The images are recorded using CCD detectors: 1024 x 1156 pixel for XUV channel, and 576 x 768 pixels for Mg XII and Fe XXV channels. Both imaging instruments have capability of observing in "Disk" mode and in "Flare" mode.

In "Disk" mode, images of the solar disk are recorded in all channels; in "Flare" mode, the instruments wait for a flare flag signal from the x-ray spectrometer to start recording (Zhitnik *et al* 1993).

During the few months of observations, CORONAS-I returned multiwavelength observations showing millions degrees plasmas confined within arch-like magnetic field structures forming active region loops, which are the sites of such explosive events as flares and coronal mass ejections. These closed magnetic structures coexist with the nebulous regions defining the quiet sun, and with the coronal holes - tenuous regions with depleted emission carried along open magnetic field lines. In addition to these distinct large-scale magnetic structures, the solar atmosphere seen in X-rays is dotted everywhere with compact bright regions, the coronal bright points.

As part of the collaborative research effort the PI's visited the FIAN institute in Moscow, and later on, two colleagues from the CORONAS team at FIAN (Dr. Zhitnik's and Dr. Pertsev), visited the CfA. During these visits, several sets of images were selected from the archival TEREK-C data base for postprocessing. The selected sets of images were recorded using different exposure times in several spectral regions: 132/5 A (FeXXIII-XXIV), 175/9 A (FeIX-XI) and 304/20 A (HeII + SiXII).

2. Application of Image Restoration/Enhancement Algorithms to CORONAS-I Images

CORONAS-I observations contain many complex structures at different spatial scales, and the contrast between various features is often very high. The characteristics and distribution of the smallest spatial scale structures cannot be readily extracted directly from these observations, either because of limited resolution and noise in the images, or because of the high dynamic range between small-scale and large-scale structures. To improve the resolution in the images, characterize the PSF and enhance the small structure in the CORONAS-I images we applied two analysis tools: Blind Iterative Deconvolution and Image Enhancement Technique.

Blind Iterative Deconvolution (Karovska, Blundell and Habbal 1991) is an image restoration technique which can be applied to high signal-to-noise images degraded by an unknown function. This technique finds a pair of functions corresponding to the degrading function and the undegraded image, which when convolved reproduce the input image within given physical constraints. A necessary condition is that the degrading function is invariant over the image field, and the degradation is linear operation. To satisfy these conditions we applied the BID to selected small regions from the images of the full Sun containing compact bright features.

Figure 1 (left) shows an example of a region selected from the full-frame TEREK-C

1024x1152 pixels image recorded in 175A (FeIX-XI) on 5/02/1993 at UT 22:21. The region was selected in the center of the Solar disk. Figure 1 (right) shows the restored image using the BID technique. The reconstructed PSF is shown in Figure 2. The PSF is slightly larger than one pixel (4 arcseconds), and therefore the deconvolution process could not produce a dramatic improvement of the resolution, although it did converge to a solution.

We also developed an image enhancement algorithm (IEA) to sharpen low-contrast small-scale structures, particularly when they are embedded in large bright structures on the disk, or located at or above the solar limb. It is based on a modified version of an algorithm that calculates the maxima of the multi-directional second derivatives of the intensities in a given image (Koutchmy et al. 1988; Karovska, Blundell, and Habbal 1994). Our algorithm detects the location of a significant change in grey level in the image by calculating the maxima of the multidirectional second derivatives. Although this method strictly speaking does not improve the resolution in the images, the sharpening of the fine structure allows detailed study of the spatial characteristics and temporal variability of the small-scale structures, often hidden within the large-scale bright features in the original images. Figure 3 (right) shows the same region as in Figure 1 (shown again in Figure 3 - left) after being enhanced using the IEA. The enhanced image shows several small-scale loops that could not be easily discerned in the original images . We also applied the IEA to the multiwavelength TEREK-C images of regions at the limb. In several images we detected coronal loops extending above the limb as well as structure in the coronal holes.

We explored the dynamical evolution of the fine structures in the active regions at different temperatures and the morphology of the structures at or near the limb using a time series of multiwavelength TEREK-C images. In Figure 4, we show He II and Fe IX–XI images taken 11 minutes apart on 1994 April 15. A correction has been made to the He II image to subtract contaminating light from the second spectral order. The images in Figure 4 were enhanced and the results are shown in the lower panels of the figure. The edge-enhancement has successfully accentuated many of the structures less visible in the original images. We also looked at similar images made on the two previous days, April 13 and 14, and we constructed movies of the April 13–15 data. The movies and the edge-enhancement techniques were both useful in distinguishing real features from those created by instrumental artifacts and photon noise. The restored and enhanced images show fine loop structures in active regions, and the substructure within the coronal bright points which could be a manifestation of preferentially heated plasma.

Finally, we studied the short time-scale variability of the fine structures in the TEREC-C images, using a sequence of nine Fe IX–XI images obtained on 1994 June 2. These images were taken on average once every 38 seconds. In Figure 5, we show the sequence of images after edge-enhancement. Supergranualar boundaries appear to brighten and fade from image to image on a time-scale shorter than a minute. We also detected a small prominence eruption at the end of the sequence in the bottom left corner of the field of view.

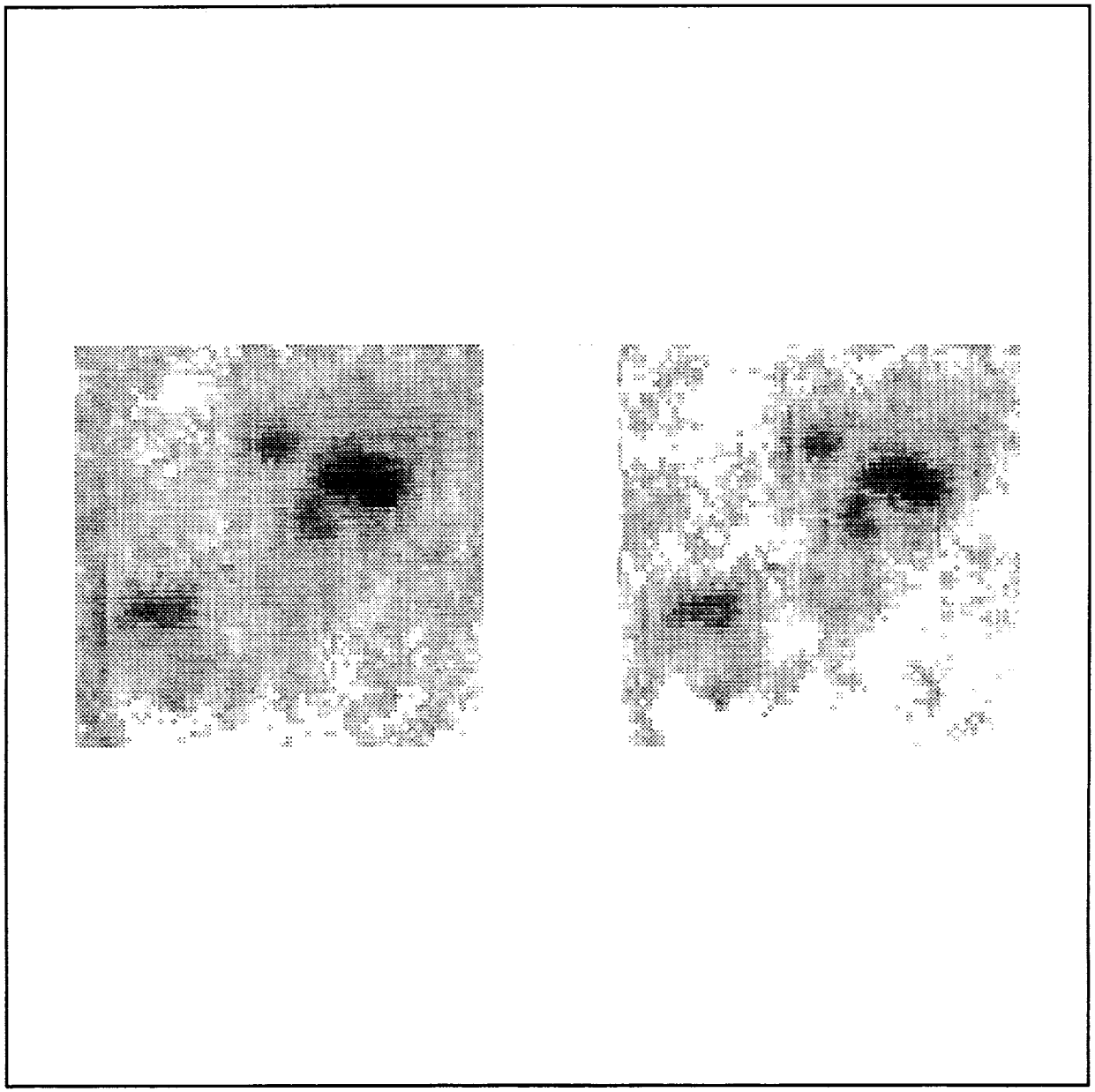

Fig. 1.— A 4 x 4 arcminutes (64 x 64 pixels) region selected from the full-frame TEREC-C 1024x1152 image recorded in 175 Å(FeIX-XI) near the center of the solar disk: (left) before the deconvolution, (right) after the deconvolution using the BID

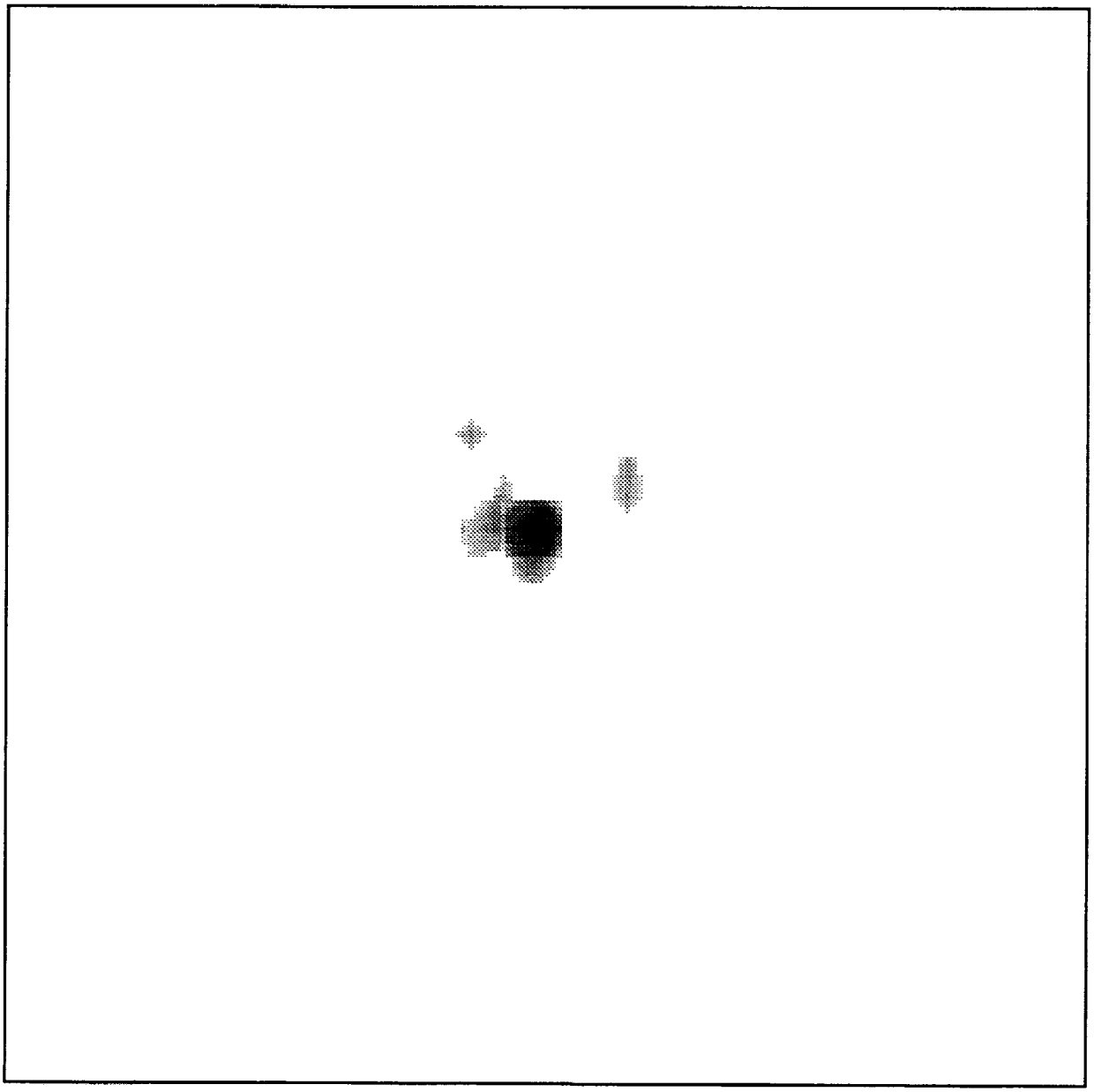

Fig. 2.— A TEREC-C PSF at 175 Å in the center of the field restored using the BID techniques. The image has been magnified to show the structure within the PSF

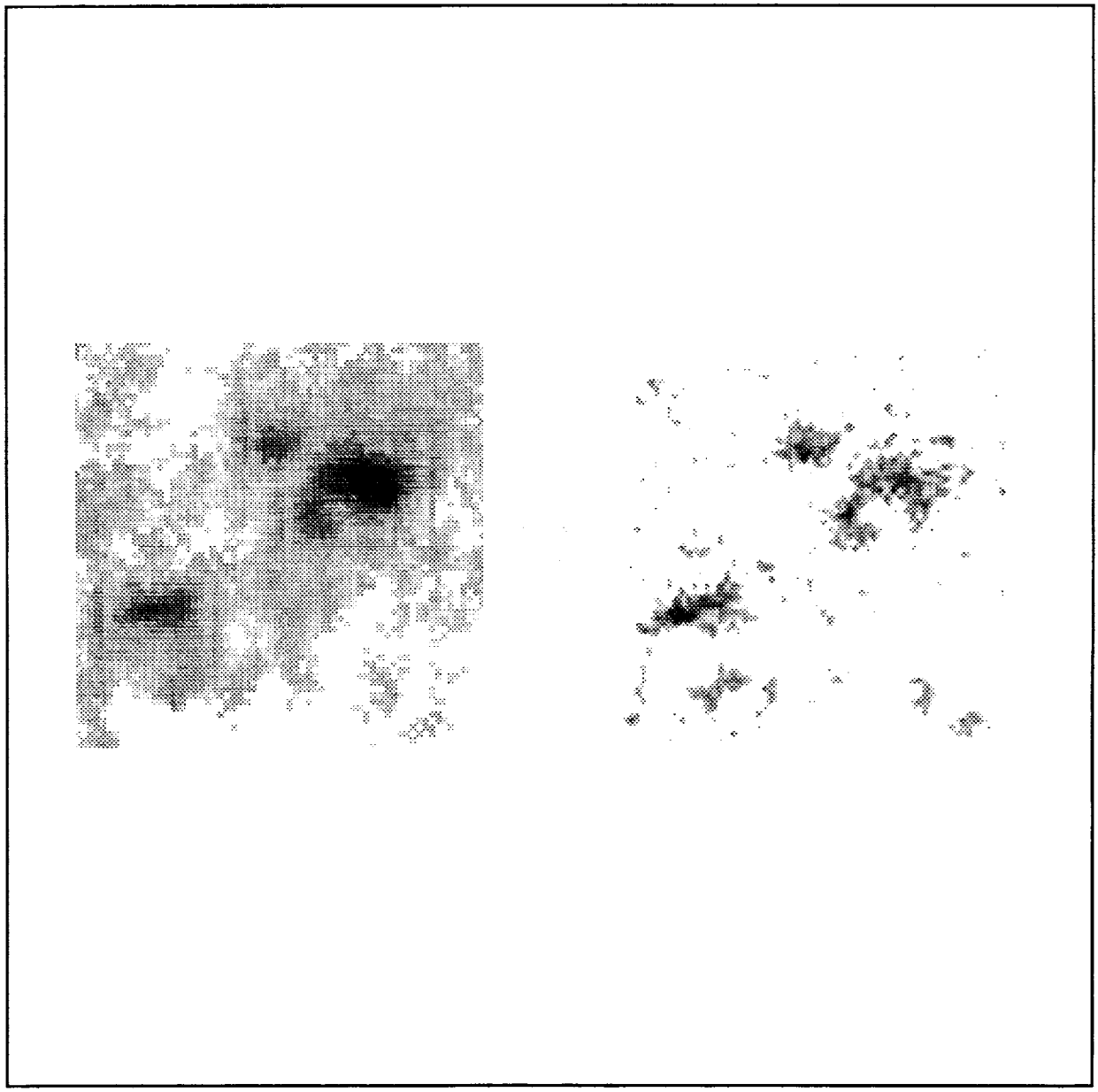

Fig. 3.— A 4 x 4 arcminutes (64 x 64 pixels) region selected from the full-frame TEREC-C 1024x1152 image recorded in 175 Å(FeIX-XI) near the center of the solar disk: (left) before the enhancement, (right) after the enhancement using the IEA

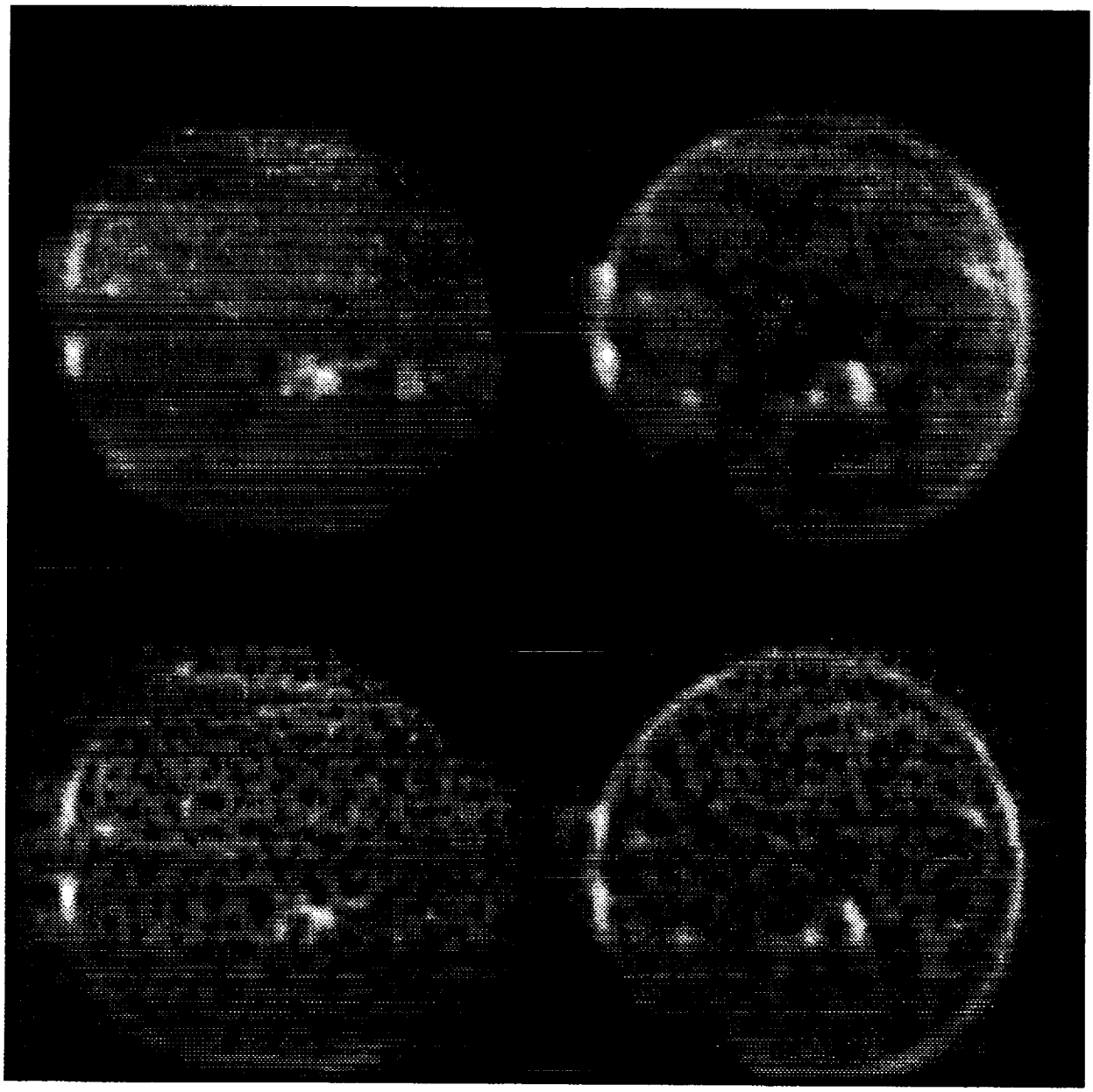

Fig. 4.— The upper panels are He II λ304 (upper left) and Fe IX–XI λ175 (upper right) CORONAS images from 1994 April 15, displayed using a square-root intensity scale. The lower panels are edge-enhanced versions of these images

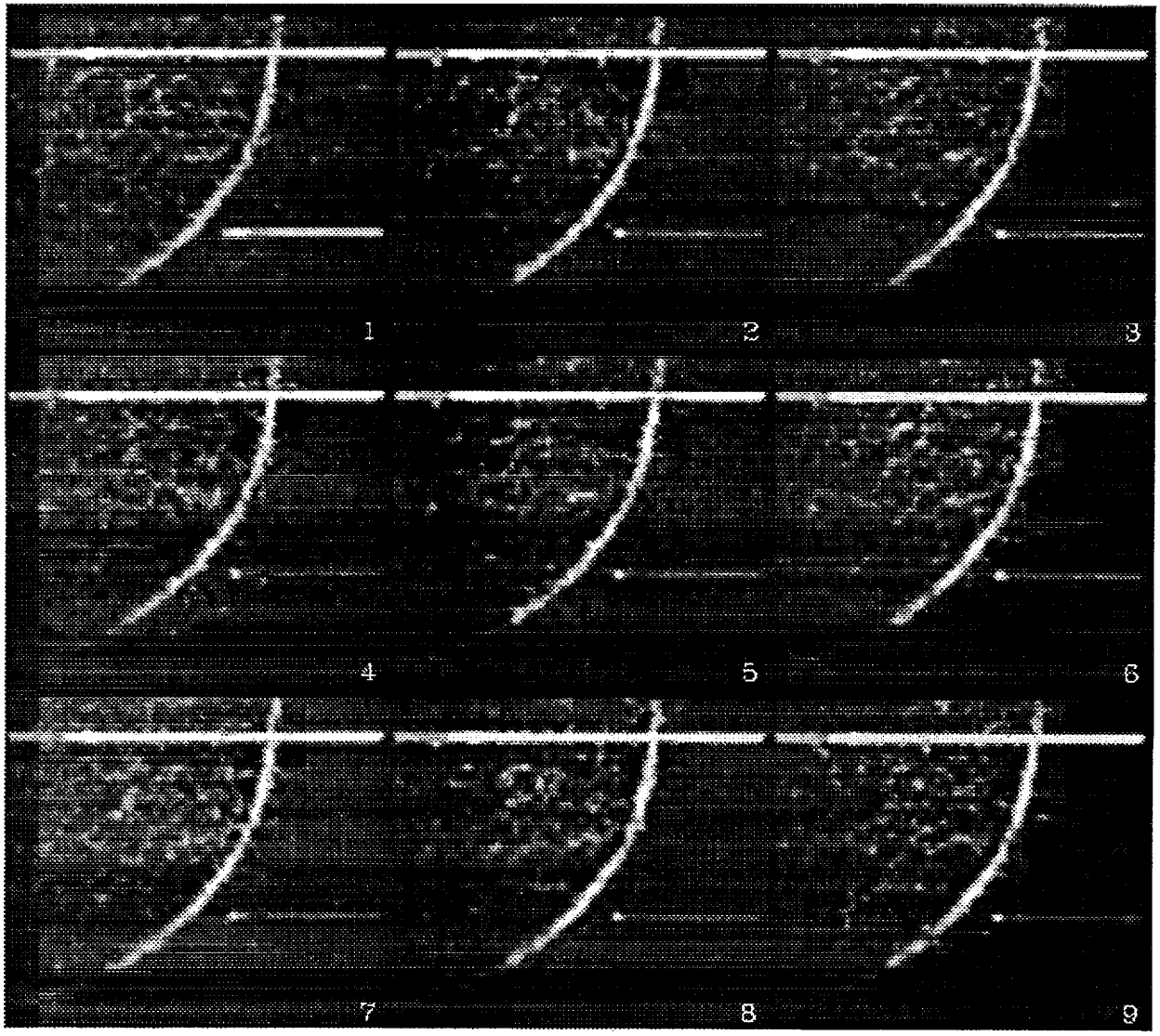

Fig. 5.— A sequence of edge-enhanced Fe IX–XI λ175 CORONAS images taken on 1994 June 2. The average time difference between the images is 38 seconds

The results of this project demonstrate the capability of image processing to substantially increase the yield from the space observations by improving the resolution and reducing noise in the images.

REFERENCES

Karovska, M., Blundell, S. F. & Habbal, S. R. 1994, ApJ, 428, 854

Koutchmy, O., Koutchmy, S., Nitschelm, C., Sykora, J. & Smartt, R. N. 1988, in the Proc. 9th Sacramento Peak Summer Symp., ed. R. C. Altrock (Sunspot: AURA), 256

Oraevsky and Zhugzhda 1991, CORONAS Information Series No. 1.

Zhitnik, I., Urnov, A., Ivanchuk, V., and Zharkova, V. eds. 1993, The CORONAS Mission: Scientific Objectives and Technical Description.

This preprint was prepared with the AAS LaTeX macros v4.0.